MICROSTRUCTURAL AND ENVIRONMENTAL EFFECTS ON FATIGUE CRACK PROPAGATION OF CONSTRUCTIONAL STEELS

M. Schaper, F. Schlät *

Investigations into the effects of microstructure and environmental factors on near-threshold fatigue crack growth are summarized. The macrocrack threshold is shown to depend on the type of microstructure, microstructural unit size, and substructural features. Environmental influences observed are those causing either excess oxidation or anodic dissolution within the crack. Related crack closure effects are a common feature. Accelerated crack growth at higher ΔK may be due to matrix embrittlement, segregated boundaries or hydrogen supply with the latter yielding frequency dependent effects.

INTRODUCTION

In metals the threshold value for fatigue crack growth (fcg), ΔK_s, is usually much smaller than the fracture toughness K_{IC}. Consistently, at near-threshold loading crack tip plastic zones are comparable in size to microstructural elements and mean growth rates of the order of the interatomic distance per cycle result. Thus, the threshold value sensitively depends on microstructure, environmental conditions, and loading variables, but often contrarily to the smooth specimen fatigue limit. At midrange fcg rates microstructure is of minor importance, whereas crack growth acceleration is reported for a large variety of environments. But despite of the research efforts focused on slow fcg major uncertainties still persist. This may be due to the complexity of the interfering effects and the experimental difficulties to be encountered. Our paper summerizes results of current investigations on slow fcg in steels and iron base alloys with particular emphasis on crack closure effects.

* Akademie der Wissenschaften der DDR, Zentralinstitut für Festkörperphysik und Werkstofforschung, Dresden

EXPERIMENTAL PROCEDURE

The materials investigated ranged from commercial steel qualities mainly of the HSLA type to high purity iron base alloys of different chemistry. Most of the ferritic pearlitic C-Mn steels which formed the basis of the experimental program were microalloyed and thermomechanically treated to achieve a variety of strength levels, grain sizes, and microstructures. The iron base alloys were doped and aged/tempered to obtain different matrix and grain boundary microstructures by varying the degree of precipitation and segregation, resp.

Unless otherwise stated the experiments were performed in laboratory air. The investigations about environmental influences were directed to hydrogen effects both in gaseous media and after/under electrolytic charging ($0{,}1N\text{-}H_2SO_4$ + 2,1mg As_2O_3/l, i =17...110A/m^2).

All the tests were conducted by means of a resonance vibration compliance technique (Schlät (1)), that proved to be especially suited for the analysis of slow growth and energy dissipation phenomena of fatigue cracks. In the DYNACOMP equipments (Schlät, Schaper (2)) the specimen represents the decisive compliance of the mechanical resonator. Thus, exciting the resonator in its exact resonance enables the effective crack length to be derived from high resolution period measurements. Using high amplitudes the resonance vibrations simultaneously serve to load the specimen and monitore its crack length. Applying non-damaging small amplitude vibrations superimposed to a quasistatically varying mean load allows the crack closure effect or low-frequency crack growth phenomena to be analysed without additional instrumentation. In the course of the experiments reported below resonance frequencies in the range 100...30Hz were used.

Threshold measurements were performed by both stepwise and continuous load shedding using reduction rates $d\Delta K/da = -1..-10 MPam^{1/2}/mm$ with the threshold value being defined for fcg rates $\Delta a/\Delta N < 5*10^{-11}$ m/cycle.Thereafter, the crack growth kinetics was measured at increasing ΔK or further threshold determinations followed.

MICROSTRUCTURAL EFFECTS

Results of the threshold measurements in our laboratory on a large variety of ferritic pearlitic steels and iron base alloys are summarized in Fig.1 (Schaper,Schlät (3)). Data of Schädlich(4) on precipitation hardenable alloys in the underaged or peak-aged conditions were ex-

cluded for clarity. Threshold values for low temperature tempered martensitic 50CrV4 and both fine and coarse grained bainitic HSLA steels from Klauss (5) and Spies et al (6) using the same technique are also shown.

Apart from the well-known trend of the threshold value to decrease with increasing strength level, Fig.1 indicates its sensitivity to the specific strengthening mechanisms applied. As an example, Fig.2 illustrates the influence of the finishing temperature, T_{EW}, on the threshold value of controlled rolled HSLA steels. Reexamining those data in terms of the ferrite grain size confirmed an inverse Hall-Petch behaviour, that could be explained on the basis of simple mechanistic models of slip band blocking at grain boundaries (3). Crack closure mechanisms can be ruled out as the primary cause of the grain size effect, which - though weaker - is also observed at a higher load ratio, where closure is known to be less significant.

The relevance of microstructural features in determining the threshold value is supported by Fig.3. In a 42 MnV 7 steel the threshold proved to be significantly higher for a coarse lamellar pearlitic microstructure as obtained by sand cooling compared to the quenched and tempered martensitic condition of approximately the same strength level (Zouhar et al (7)).

For macrocracks in coarsegrained materials the grain size dependence of the threshold value disappears (3). Thus, at large grain sizes substructural features and dislocation behaviour within the grain become important. For example, enhanced thresholds were measured in underaged FeCuNi alloys as compared to the non-aged or overaged conditions (4). Fractografic analysis revealed this to be due to crack growth along slip bands, which lead to a distinct fracture surface roughness (8).

Contrary to the grain size the grain boundary microstructure is without relevance for the threshold value. This could be confirmed by measurements on overaged FeSiTi alloys containing grain boundaries covered with large precipitates(4) as well as on FeNi alloys and HSLA steels doped with Sb and tempered at 753K/250h (8). Apart from a minor grain size dependence the threshold was unaffected by the thermal treatments applied. On the contrary, a severe degree of grain boundary embrittlement due to cosegregation of Ni+ Sb or heavily precipitated grain boundaries caused markedly enhanced fcg rates soon above the threshold. In some cases growth bursts could be identified with individual intergranular cracking events.

ENVIRONMENTAL EFFECTS

Hydrogen supply is believed to be of primary importance for accelerated fcg in aggressive environments. To further clarify some unresolved questions regarding the H-effect experiments on near-threshold fcg in C-Mn HSLA steels were performed in H containing gaseous environments and after/during electrolytic charging.

In the investigated gaseous media near-threshold fcg proved to be independent on H content, but weakly affected by their humidity. As could be shown the growth rates very near to the threshold become slightly lower when changing the environment from purified hydrogen or dry Ar to technical N_2, O_2, or air of usual moisture. Related effects on the threshold value are only week. Minor differences in the amount of fretting oxidation in the wake of the crack are suggested to explain this behavior. In water vapor saturated air, however, the threshold is markedly enhanced (Fig.4) due to excess oxidation with macroscopically observable thick corrosion products on both crack faces. Similarily, under sustained load the built-up of corrosion products within the crack could be elucidated by a time dependent diminuition of the specimen compliance.

At higher ΔK accelerated fcg was measured in H containing atmospheres (Fig.5). Order of magnitude enhancements of the local and mean fcg rates are obviously due to cyclic cleavage and could be shown to be connected with a reduced specific energy dissipation U (3). Competing H and residual O adsorption rates are suggested to be responsible for the observed influence of the H gas purity. Furthermore, the frequency depen-dence of the H effect points to the fresh surface production and H diffusion rates as important factors.

The importance of the H diffusion rate is further supported by the tests performed following as well as during electrolytic charging the specimen with H (Fig.6, 7). In both cases distinctly enhanced fcg rates were measured on loading at frequencies as low as 0,05Hz as compared to about 50Hz. On the other hand, In laboratory air only a very small frequency effect was observed which is believed to be due to the thermally activated nature of the dislocation processes. From economic reasons no low frequency tests were performed at very low fcg rates. At the higher frequencies a small plateau appeared in the transition from the threshold to Paris region, where either trans- or intergranular facets are usually observed in air.The most remarkable feature,how-

ever, is a monotonically decreasing fcg rate during load shedding under kathodic polarization in the electrolyte. The threshold is markedly reduced, at least below that value measured in air at high load ratio. The offset in Fig.7 between decreasing and increasing load sequences as well as fractografic evidence strongly suggest anodic dissolution processes as the underlying mechanism.

CRACK CLOSURE

Attempts to explain the effect of microstructure, environment, and loading conditions on near-threshold fcg must include the phenomenon of crack closure at positive applied loads. A typical example for such premature crack closure is shown in Fig.8 for low and high load ratios at successive loading stages. The evaluation of an K_{op} in the transition from partial closure to the fully opened crack, where the effective crack length equals the real one, is often used to normalize near-threshold growth curves in terms of an $\Delta K_{eff} = K_{max} - K_{op}$, if $K_{op} > K_{min}$. This simple interpretation of the closure effect neglects its gradual nature and implys zero damage ahead of the crack tip below K_{op}. Therefore, in spite of the principle mechanisms being well documented the mechanistic consequences of the crack closure effect are not generally accepted.

In the course of our investigations sophisticated measurements (8) and in-situ experiments in the SEM (10) clearly revealed the role of fracture path tortuosity and corrosion deposits in promoting crack closure at near-threshold and low R loading. The resulting increase of the specific energy dissipation, U,near the threshold is documented by Fig.9 for a commercial HSLA steel. Evidence for a strong correlation between pronounced crack closure and enhanced threshold values has been obtained for FeCuNi alloys in the underaged condition, where near-threshold cracks propagated along slip bands and produced a rough surface topography (8). An example for environmentally induced closure effects is shown in Fig. 10a. Obviously, the higher closure level in water vapor saturated air is due to excess corrosion deposits within the crack and corresponds to the enhancement of the thre shold value depicted in Fig.4. On the contrary, anodic dissolution processes are suggested to be the cause for the largely suppressed closure effect (Fig.10b) and the simultaneous diminuition of the threshold value (Fig.7). Thus, in spite of the current limitations of the crack closure concept, obviously, microstructural and environmental conditions yielding large threshold effects are often conected with alterations in the closure behaviour

SYMBOLS USED

a, a_{eff} = real, and effective crack length (mm)

$\Delta a/\Delta N$ = crack propagation rate (m/cycle)

$K, \Delta K, K_{op}$ = mean, cyclic, and crack opening stress intensity, resp., (MPa*m1/2)

$d\Delta K/da$ = ΔK reduction per crack growth increment ($MPa*m^{1/2}/mm$)

U = specific energy dissipation per unit area of crack growth (J/m^2)

REFERENCES

(1) Schlät,F., Int.J.Fracture, Vol.19,1982,pp.R37-40
Neue Hütte, Vol.27,1982,pp.146-149

(2) Schlät,F.,and Schaper,M., Proc."9th Congress on Materials Testing", Ed.by E.Czoboly, Technoinform, Budapest,1986, Vol.1,pp.109-113

(3) Schaper,M. and Schlät,F., Proc. Int.Colloquium "Basic Mechanisms in Fatigue of Metals", Brno,CSSR 1988, Ed.by P.Lukas, Elsevier and Academia

(4) Schaper,M., Schädlich,S. et al, Proc.6th Symp. "Verformung und Bruch", Magdeburg,DDR, 1982, Vol.2, p.57, and Schädlich,S., Dissertation, AdW der DDR

(5) Klauss,H.-J., unpublished work

(6) Spies,H.-J., Hübner,P., and Pusch,G., in "Festigkeitsverhalten höherfester schweissbarer Baustähle" Verl.Grundstoffindustrie, Leipzig,DDR,1984,pp.72-93

(7) Zouhar,G., et al, Proc.7th Symp."Verformung und Bruch", Magdeburg, DDR, 1985, Vol.2

(8) Schaper,M., and Schlät,F., Proc.6th Int.Coll."Mechanical Fatigue of Metals", Miskolc, Hungary,1983, in Publ.Techn.Univ.Miskolc, Vol.C 39, pp.173-187

(9) Bösel,D.,and Schaper,M., Proc.5th Symp."High Purity Materials in Science and Technology", Dresden,1985, AdW der DDR, Vol. P2, pp.356-358

(10) Schaper,M., and Bösel,D., Prakt.Metallografie, Vol.22, 1985, pp.197-203

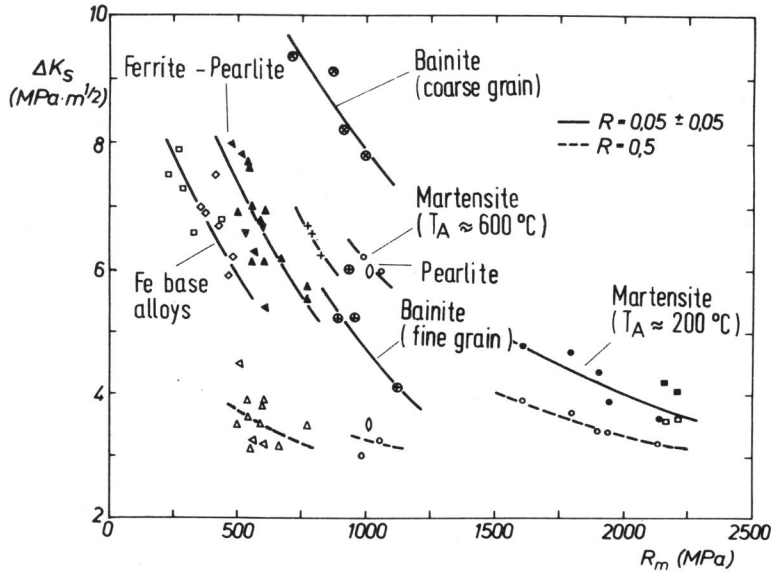

Figure 1. Fatigue crack propagation threshold for steels and iron base alloys, effect of strength level

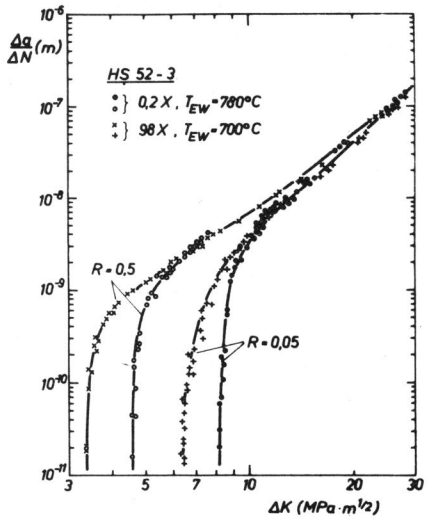

Figure 2. Effect grain size on fcg, HSLA steel

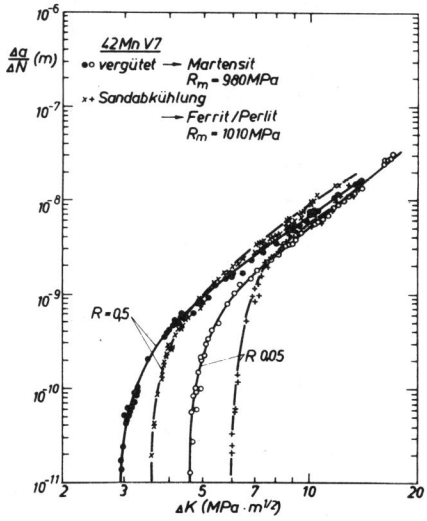

Figure 3. Effect of cooling rate on fcg, 42MnV7 steel

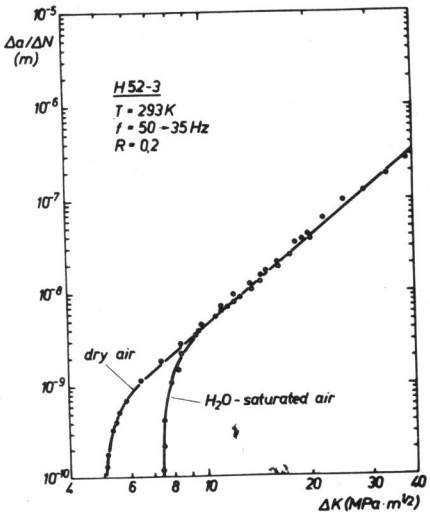

Figure 4. Near-threshold fcg in water vapor saturated air

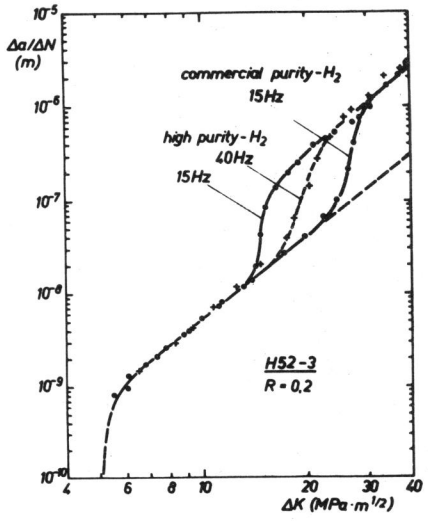

Figure 5. Accelerated fcg in gaseous environments

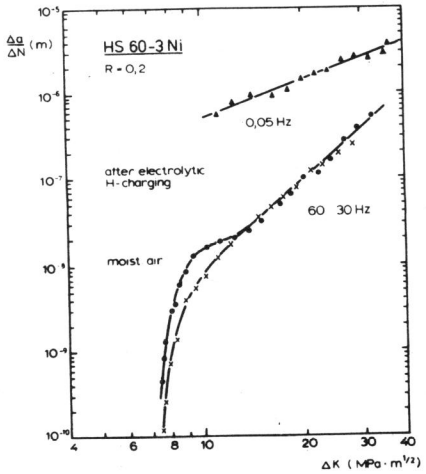

Figure 6. Influence of prior electrolytic charging on fcg

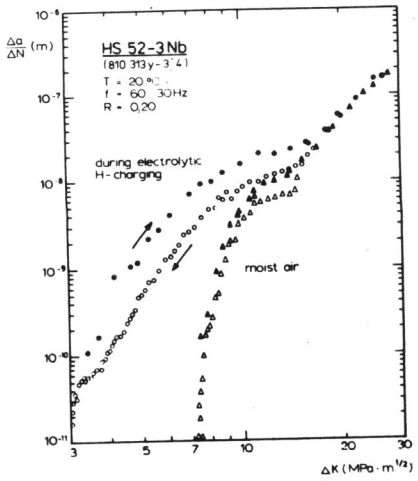

Figure 7. Slow fcg during electrolytic H-charging

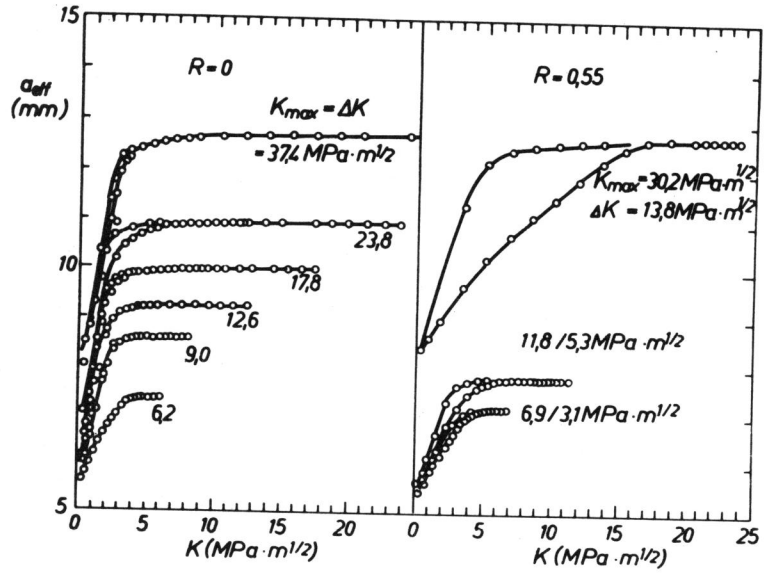

Figure 8. Crack closure during fcg in successive load stages at two different load ratios, HSLA steel, air

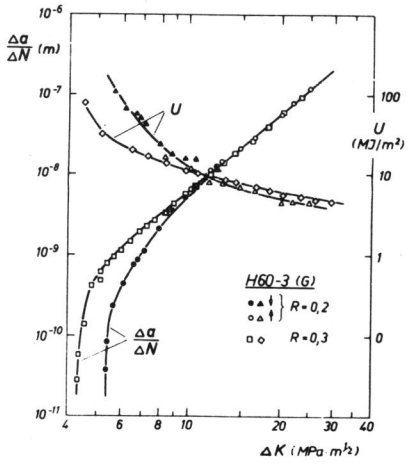

Figure 9. Specific energy dissipation at slow fcg

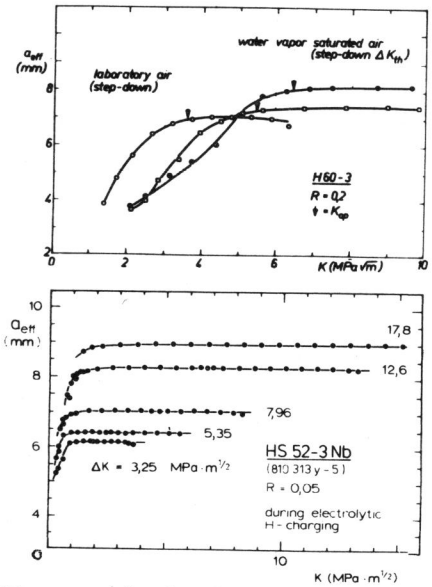

Figure 10a,b. Environmental effects on crack closure